

Flight muscles degenerate by programmed cell death after migration in the wheat aphid, *Sitobion avenae*

Honglin Feng (✉ hf329@cornell.edu)

<https://orcid.org/0000-0001-6803-3413>

Xiao Guo

Chongqing Academy of Agricultural Sciences

Hongyan Sun

University of Miami

Shuai Zhang

Chinese Academy of Agriculture Sciences

Jinghui Xi

Jilin University

Jiao Yin

Chinese Academy of Agricultural Sciences

Yazhong Cao

Chinese Academy of Agricultural Sciences

Kebin Li

Chinese Academy of Agricultural Sciences Institute of Plant Protection

Research note

Keywords: aphid, *Sitobion avenae*, flight muscle, ubiquitin, programmed cell death

Posted Date: October 15th, 2019

DOI: <https://doi.org/10.21203/rs.2.13011/v3>

License:  This work is licensed under a Creative Commons Attribution 4.0 International License.

[Read Full License](#)

Version of Record: A version of this preprint was published on October 21st, 2019. See the published version at <https://doi.org/10.1186/s13104-019-4708-z>.

Abstract

Objective Previous studies showed that flight muscles degenerate after migration in some aphid species; however, the underlying molecular mechanism remains virtually unknown. In this study, using the wheat aphid, *Sitobion avenae*, we aim to investigate aphid flight muscle degeneration and the underlying molecular mechanism. Results *S. avenae* started to differentiate winged or wingless lines at the second instar, the winged aphids were fully determined at the third instar, and their wings were fully developed at the fourth instar. After migration, the aphid flight muscles degenerated via programmed cell death, which is evidenced by a Terminal deoxynucleotidyl transferase dUTP-biotin nick end labeling assay. Then, we identified a list of differentially expressed genes before and after tethered flights using differential-display reverse transcription-PCR. One of the differentially expressed genes, ubiquitin-ribosomal S27a, was confirmed using qPCR. Ubiquitin-ribosomal S27a is drastically up regulated following the aphids' migration and before the flight muscle degeneration. Our data suggested that aphid flight muscles degenerate after migration. During flight muscle degeneration, endogenous proteins may be degraded to reallocate energy for reproduction.

Introduction

Many aphids develop wing polyphenism, and winged aphids explore new habitats by migration (1). After winged aphids migrate to new host plants and/or the onset of larviposition, the indirect flight muscles (IFM) degenerate (2-6).

IFM degeneration has been previously depicted as regulated processes in insects including some aphids (7, 8). The regulation of IFM degeneration involves multiple factors: juvenile hormone (JH); neural factors; and specific proteins. (i) JH treatment induces IFM degeneration (8-10). (ii) Denervated muscles in the presence of JH initiated degeneration earlier than the innervated muscles in cricket (11). (iii) specific proteins are induced despite the overall decreases of protein synthesis. Ubiquitin, a marker for programmed cell death (PCD), accumulates when aphid IFM undergoes degeneration (7, 8). Although IFM degeneration has been suggested as an active PCD, the underlying molecular mechanism remains unclear.

The wheat aphid, *Sitobion avenae*, migrates from southern to northern China and causes ~10% wheat yield losses every year (12). Here, we investigated *S. avenae* wing development and IFM degeneration, and identified some differentially expressed genes pre-/post-migration. We further analyzed the dynamic expression of ubiquitin-ribosomal S27a (*RPS27a*) during IFM degeneration.

Methods

Aphids

We generated an isogenic *S. avenae* population using a single wingless aphid. Aphids were raised on wheat seedlings at 22°C with a 16h/8h light/dark photoperiod. Winged aphids were obtained by

manipulating aphid densities. Under low-density, one wingless aphid was reared on a joint-stage wheat to maintain the wingless morph. Under high-density, 80 wingless adult aphids were reared on one ripe wheat to induce the winged morph (6).

To investigate IFM degeneration, we collected the winged aphids every 24h from eclosion (0 day), to migration (5th day), to reproduction (8th day), until death was observed. For each timepoint, half of the aphids were collected for morphological, histological, and apoptosis examinations. The other half were dissected for qPCR following a freeze-drying procedure (13).

Morphological examination

We examined the external morphology of aphid thorax using scanning electron microscope (SEM). Aphids were fixed in 3% glutaraldehyde for 24hrs and transferred to 1% osmic acid. Then aphids were saturated with ethanol, exchanged using isopentyl acetate, and dried in a Hitachi CO₂ Critical Point Dryer. Aphids were then coated with gold in a sputter coater (Hitachi, IB-5) and imaged under a Hitachi S-570 SEM.

We examined the internal morphology of aphid thorax using histological staining. Aphids were fixed in 4% paraformaldehyde for 4hrs. The specimens were dehydrated in a serial of ethanol solutions (70%, 80%, 90%, 100%, 10 mins/each), cleared in xylene, and embedded in paraffin. Serial sections were cut and stained with hematoxylin and eosin for imaging using a Carl Zeiss Primo Star Microscope.

Terminal deoxynucleotidyl transferase dUTP-biotin nick-end labeling (TUNEL) assay

To examine apoptosis, we performed a TUNEL assay using an *in-situ* apoptosis detection kit (Boster, China). Briefly, paraffin-embedded aphids were sliced into 5μm sections, which were rehydrated in xylene for 20 mins and a serial of ethanol solutions (100%, 90%, 80%, 70%, 10 mins/each). Then all specimens were permeabilized using Proteinase K (1:200) for 10 mins and quenched using 3% H₂O₂ for 10 mins. Quenched specimen were labeled with TdT Labeling Reaction Mix (TdT:DIG-dUTP:Buffer=1:1:18) for 2hrs at 25°C. After wash with 0.01M TBS buffer, specimens were incubated with anti-DIG antibody (1:100) for 30 mins. Specimens were then incubated with SABC (1:100) for 30 mins and with Diaminobenzidine for 15 mins, then counterstained with Hematoxylin for 3 mins. Finally, specimens were washed with 100% ethanol, 100% xylene, and mounted for imaging.

Previous study suggested that feeding induces JH secretion, which triggers IFM degeneration (5). Therefore, we examined the IFM degeneration on fasted aphid as a control. For fasting, winged aphids were transferred to water-soaked sponges. Every 6hrs, aphids were transferred to rearing plants for 2hrs to avoid death.

Differential-display reverse transcription-PCR (DDRT-PCR)

To identify differentially expressed genes pre-/post-migration, we performed tethered flight using 3-4 days post-eclosion aphids. For pre-migration, aphids were tethered (not flighted) and flash-frozen. For post-migration, aphids were tethered and flighted for 24hrs using a flight-mill program (14); flighted aphids were flash-frozen.

Total RNA was extracted from single aphid using Easy-Spin Total RNA Rapid Extraction Kit (Biomad) and reverse-transcribed by PrimeScript™ 1st-Strand cDNA Synthesis Kit (Takara). For DDRT-PCR, we designed three one-base anchored oligo-dT 3' primers and eight arbitrary 5' primers (13-mers) according to the GenHunter RNAimage DD Kit (3x8 pairs) (Table S1). Each PCR reaction was composed of 10 μ l 2X PCR mix, 1 μ l 5' primer, 1 μ l 3' primer, 2 μ l cDNA, and 6 μ l ddH₂O. The PCR program was 94°C for 1 min, followed by 30 cycles of 94°C for 30s, 48°C for 1 min and 72°C for 1 min, and a final extension step at 72°C for 5 min. Then 2 μ l PCR products of each reaction were used as template for a second round of PCR. The final PCR products were visualized using 6% SDS polyacrylamide gel electrophoresis (Fig S2).

Differentially expressed genes were excised for sequencing, obtained sequences were annotated on NCBI.

RPS27a dynamic expression

The sequence of *S. avenae* *RPS27a* was obtained using a rapid amplification of cDNA ends method (3'-RACE). Partial *S. avenae* *RPS27a* sequence containing the start codon was amplified using Ub-F/Ub-R primers designed based on *A. pisum* *RPS27a*. The complete C-terminal of *RPS27a* was obtained using a RACE kit (Takara) with gene specific primers and the kit-provided outer/inner primers (Table S2). To check the conservation of *RPS27a*, the nucleotide and deduced amino acid sequences were aligned with homologous from other insects using DNAMAN (Fig S3).

We quantified the *RPS27a* expression during IFM degeneration using qPCR in tissues including head, thorax, and abdomen. Briefly total RNA was extracted from tissues pooled from ~10 aphids, then same amount of RNA (0.1 μ g) for each sample was used for cDNA Synthesis. The qPCR reaction was 25 μ l containing 12.5 μ l 2*PCR SuperMix, 0.5 μ l Passive Reference DYE, 0.5 μ l of each qPCR primer (Table S2), 1 μ l cDNA and ddH₂O. The qPCR program was 2 min at 95°C followed by 45 cycles of 15s at 95°C, 15s at 55.5°C and 30s at 72°C, and then melt curve under 55-95°C 0.5°C + (80 cycles). To calculate gene expression, a credible standard curve was constructed using a series of 10x dilutions of a standard sample. Each experiment included 3-4 technical replicates for each sample and repeated three times.

Results

Flight muscle development in S. avenae

The external and internal structures were similar in the winged and wingless aphids at the 1st instar; wing primordia were observed in the internal structures of both morphs (Fig S1A, a). From the 2nd instar, wing primordia developed and enlarged in the winged morph, but disappeared in the wingless morph (Fig S1b, b'). At the 3rd instar of wing aphids, swollen structures appeared and later developed into wing bud (Fig S1C, C'). IFM fibers also differentiated; the corresponding area was occupied by fat bodies in the wingless morph hereafter (Fig S1c, c'). To the 4th instar, wing buds enlarged into a plate shape and the wing epithelia were folded in a complicated structure, differentiating the forewings and hindwings (Fig S1d'). To adults, the wings were fully developed; wing hair sensilla were also seen in the winged morph (Fig S1E, F).

IFM degeneration after S. avenae migration

The IFM of an alatae adult was plump at the 1st day after eclosion till the 5th day (Fig 1A, 1B). From the 9th day, the IFM started to degenerate. The myofibrils appeared to be thin. The diameter of the myofibrils was reduced, and the volume of the interfibrillar sarcoplasmic region increased (Fig 1C); the degradation continued through the 11th day (Fig 1D). To the 13th day, the IFM was degenerated completely (Fig 1E). The contractile fiber vanished, and the intact IFM was not visible.

IFM degeneration after migration is PCD

In sections of aphid pterothorax stained in the TUNEL experiment, no apoptotic signals were observed in alatae aphid before the 7th day after eclosion (Fig 2A). The first apoptotic signal appeared in aphids at the 7th day as brownish yellow grains (Fig 2B), which is similar to the apoptosis signals in the positive controls (Fig 2C, C'). In parallel, we did not find any apoptotic signals in the muscles of the 3rd, and 7th day fasted aphids (Fig 2A', B').

Differentially expressed genes pre-/post-migration

We identified 36 differentially expressed genes that were classified into three groups (Table S3): 1) genes related to apoptosis: this group includes the widely studied apoptotic genes like p53 regulator (15) and the apoptosis marker, *RPS27a* (7, 8); Some additional genes are related to apoptosis in specific conditions. Ras-related protein Rab-29B regulates lysosome integrity related to age associated defects (16). 2) genes related to metabolism: this group includes genes in metabolism of amino acids (e.g. D-amino acid dehydrogenase), sugars (e.g. glucose transporter 1), and vitamins (e.g. 3,4-dihydroxy-2-butanone-4-phosphate synthase). Genes important to energy re-allocation were also found differentially

expressed, including exocyst complex component 3 (17) and serpin 3a (18). 3) genes with unknown functions.

S. avenae RPS27a dynamic expression

The *S. avenae RPS27a* encodes a 150 aa protein (76aa ubiquitin + 74aa ribosomal protein). The sequences of *RPS27a* are highly conserved across different insects (84-93.3%), and the divergence was mainly from the ribosomal protein, whereas the ubiquitin monomers were almost identical (Fig S3).

The expression of *S. avenae RPS27a* changed dynamically pre/post IFM degeneration. Initially after eclosion, *RPS27a* remained a constant low expression in head, thorax, and abdomen (Fig 3). The expression started raising from the 3rd day post-eclosion. *RPS27a* expression significantly increased and was significantly higher in abdomen than head and thorax in the 6th day, which is one day post-migration and one day before the apoptotic signals were detected (Fig 2C). After aphid migration, a sharp decrease of *RPS27a* occurred in the 7th day (Fig 3), the day that apoptosis signals were detected (Fig 2C).

Discussion

IFM degeneration has been mostly studied physiologically in insects such as fruit fly, crickets, bugs, and some aphids (7, 19-25). Here, we depicted the IFM development and degeneration in *S. avenae* and identified genes that may regulate IFM degeneration.

IFM degeneration for energy re-allocation

A trade-off has been proposed between IFM degeneration and reproduction with regard to energy allocation (26). IFM degeneration is regulated in many insects, and the products are reallocated to reproduction (24-30). Here, we identified two groups of genes that differentially expressed pre-/post-aphid migration (Table S3). First group included apoptotic genes, like Ras-related Rab-29b, p53, and RPS27a, which suggested that aphid IFM degeneration is an active PCD. The second group included metabolic genes. Some of those genes are involved in the metabolism of energy building blocks (e.g. amino acids, sugars, and vitamins), while other genes are involved in energy transport (e.g. exocyst complex component-3). The differentially expressed genes indicated that aphid IFM degeneration is an active process that involves a trigger of PCD followed by a systematic reallocation of energies (e.g. from migration to reproduction) (5, 29, 31, 32).

Ubiquitin functions as a marker for aphid IFM degeneration

Ubiquitin degrades proteins in eukaryotic cells. During cell apoptosis, short-lived proteins are subjected to ubiquitination, which triggers different degenerative processes (33, 34). Here, we found that the *S. avenae* *RPS27a* was significantly differentially expressed pre-/post aphid migration. *RPS27a* showed a sharp increase before aphid migration and a sudden decrease after migration, which indicated that *RPS27a* is programmed during IFM degeneration. *RPS27a* may function as a trigger for apoptosis to regulate IFM degeneration (33-35) or *RPS27a* may degenerate waste proteins to facilitate energy reallocation (36). Interestingly, from our qPCR results, *RPS27a* was primarily expressed in abdomen compared to head and thorax. During IFM degeneration, *RPS27a* may trigger a systematic energy reallocation during the shift from migration to reproduction; *RPS27a* functions as a general protein degradation machinery throughout aphid body including abdomen, which is the major energy sink for reproduction.

Limitations

The timing of migration and IFM degeneration determines whether insects can locate preferable host plants (37). We investigated the IFM degeneration using tethered flight system on lab aphid population. However, the timing of aphid migration and IFM degeneration in nature remains elusive.

Abbreviations

RPS27a: ubiquitin-ribosomal S27a; IFM: Indirect flight muscles; JH: Juvenile hormone; TUNEL: Terminal deoxynucleotidyl transferase dUTP-biotin nick-end labeling assay; DDRT-PCR: Differential-display reverse transcription-PCR; SEM: Scanning electron microscope; PCD: Programmed cell death; RACE: Rapid amplification of cDNA ends.

Declarations

Ethics approval and consent to participate

Not applicable.

Consent for publication

Not applicable.

Availability of data and materials

All data generated or analyzed during this study are included in this published article and its supplementary information files.

Competing interests

The authors declare that they have no competing interests.

Funding

This work was supported by the National Key R&D Program of China (Grant No. 2017YFD0201700), National Special Fund for Scientific Research on Public Causes (Grant No.200803002) and the Public Welfare Project from Ministry of Agriculture of the People's Republic of China (Grant No.201103022). Funding agencies had no role in the design of the study and collection, analysis, and interpretation of the data, or writing of the manuscript.

Authors' Contributions

HF, XG, KL and YC conceived of the study, HF, XG, HS, JX, and JY designed the experiments. HF, XG, HS, and SZ performed the experiments and data analysis. HF, XG, and KL wrote the manuscript. All authors contributed to preparation of the final version of the manuscript. All authors read and approved the final manuscript.

Acknowledgements

Not applicable.

References

1. Kennedy JS. Aphid migration and the spread of plant viruses. *Nature*. 1950;165(4208):1024-5.
2. Johnson B. Studies on the degeneration of the flight muscles of alate aphids-I:A comparative study of the occurrence of muscle breakdown in relation to reproduction in several species. *Journal of Insect Physiology*. 1957;1(3):248-50.
3. Johnson B. Studies on the degeneration of the flight muscles of alate aphids-II: Histology and control of muscle breakdown. *Journal of Insect Physiology*. 1959;3(4):367-72.
4. Johnson B. An electron microscopic study of flight muscle breakdown in an aphid *Megoura viciae*. *Tissue Cell*. 1980;12(3):529-38.
5. Kobayashi M, Ishikawa H. Breakdown of indirect flight muscles of alate aphids (*Acyrtosiphon-Pisum*) in relation to their flight, feeding and reproductive-behavior. *Journal of Insect Physiology*. 1993;39(7):549-54.
6. Ishikawa A, Miura T. Differential regulations of wing and ovarian development and heterochronic changes of embryogenesis between morphs in wing polyphenism of the vetch aphid. *Evolution & Development*. 2009;11(6):680-8.
7. Kobayashi M, Ishikawa H. Mechanisms of histolysis in indirect flight muscles of alate aphid (*Acyrtosiphon-Pisum*). *Journal of Insect Physiology*. 1994;40(1):33-8.
8. Kobayashi M, Ishikawa H. Involvement of juvenile-hormone and ubiquitin-dependent proteolysis in flight muscle breakdown of alate aphid (*Acyrtosiphon-Pisum*). *Journal of Insect Physiology*. 1994;40(2):107-11.

9. Selma-Soriano E, Artero R, Llamusi B. Optical Cross-Sectional Muscle Area Determination of *Drosophila Melanogaster* Adult Indirect Flight Muscles. *Journal of Visualized Experiments*. 2018;133.
10. Oliver RH, Albury AN, Mousseau TA. Programmed cell death in flight muscle histolysis of the house cricket. *Journal of Insect Physiology*. 2007;53(1):30-9.
11. Shiga S, Yasuyama K, Okamura N, Yamaguchi T. Neural- and endocrine control of flight muscle degeneration in the adult cricket, *Gryllus bimaculatus*. *Journal of Insect Physiology*. 2002;48(1):15-24.
12. Hu XS, Liu YJ, Wang YH, Wang Z, Yu XL, Wang B, et al. Resistance of wheat accessions to the English grain aphid *Sitobion avenae*. *PLoS One*. 2016;11(6):e0156158.
13. Fujita SC, Inoue H, Yoshioka T, Hotta Y. Quantitative tissue-isolation from *Drosophila* freeze-dried in acetone. *Biochem J*. 1987;243(1):97-104.
14. Cheng D, Tian Z, Li H, Sun J, Chen J. Influence of temperature and humidity on the flight capacity of *Sitobion avenae*. *Acta Entomologica Sinica*. 2002;45(1):80-5.
15. Aubrey BJ, Kelly GL, Janic A, Herold MJ, Strasser A. How does p53 induce apoptosis and how does this relate to p53-mediated tumour suppression? *Cell Death and Differentiation*. 2018;25(1):104-13.
16. Kuwahara T, Inoue K, D'Agati VD, Fujimoto T, Eguchi T, Saha S, et al. LRRK2 and RAB7L1 coordinately regulate axonal morphology and lysosome integrity in diverse cellular contexts. *Sci Rep-Uk*. 2016;6.
17. Barkefors I, Fuchs PF, Heldin J, Bergstrom T, Forsberg-Nilsson K, Kreuger J. Exocyst Complex Component 3-like 2 (EXOC3L2) Associates with the Exocyst Complex and Mediates Directional Migration of Endothelial Cells. *J Biol Chem*. 2011;286(27):24189-99.
18. Aguilera S, Izquierre G, Martinez-Martinez I, Vicente V, Olson ST, Corral J. Disease-causing mutations in the serpin antithrombin reveal a key domain critical for inhibiting protease activities. *J Biol Chem*. 2017;292(40):16513-20.
19. Piccirillo R, Demontis F, Perrimon N, Goldberg AL. Mechanisms of muscle growth and atrophy in mammals and *Drosophila*. *Developmental Dynamics*. 2014;243(2):201-15.
20. Zera AJ, Larsen A. The metabolic basis of life history variation: genetic and phenotypic differences in lipid reserves among life history morphs of the wing-polymorphic cricket, *Gryllus firmus*. *Journal of Insect Physiology*. 2001;47(10):1147-60.
21. Zhao Z, Zera AJ. A morph-specific daily cycle in the rate of JH biosynthesis underlies a morph-specific daily cycle in the hemolymph JH titer in a wing-polymorphic cricket. *Journal of Insect Physiology*. 2004;50(10):965-73.
22. Zhao ZW, Zera AJ. The hemolymph JH titer exhibits a large-amplitude, morph-dependent, diurnal cycle in the wing-polymorphic cricket, *Gryllus firmus*. *Journal of Insect Physiology*. 2004;50(1):93-102.
23. Zera AJ. Intermediary metabolism and life history trade-offs: lipid metabolism in lines of the wing-polymorphic cricket, *Gryllus firmus*, selected for flight capability vs. early age reproduction. *Integr Comp Biol*. 2005;45(3):511-24.

24. Socha R, Sula J. Flight muscles polymorphism in a flightless bug, *Pyrrhocoris apterus* (L.): Developmental pattern, biochemical profile and endocrine control. *Journal of Insect Physiology*. 2006;52(3):231-9.
25. Socha R, Sula J. Differential allocation of protein resources to flight muscles and reproductive organs in the flightless wing-polymorphic bug, *Pyrrhocoris apterus* (L.) (Heteroptera). *J Comp Physiol B*. 2008;178(2):179-88.
26. Lorenz MW. Oogenesis-flight syndrome in crickets: age-dependent egg production, flight performance, and biochemical composition of the flight muscles in adult female *Gryllus bimaculatus*. *Journal of Insect Physiology*. 2007;53(8):819-32.
27. Tanaka S. Effects of wing-pad removal and corpus allatum implantation on development of wings, flight muscles, and related structures in the striped ground cricket, *Allonemobius-Fasciatus*. *Physiol Entomol*. 1985;10(4):453-62.
28. Tanaka S. De-alation, flight-muscle histolysis, and oocyte development in the striped ground cricket, *Allonemobius-Fasciatus*. *Physiol Entomol*. 1986;11(4):453-8.
29. Nair CRM, Prabhu VKK. Entry of proteins from degenerating flight muscles into oocytes in *Dysdercus Cingulatus* (Heteroptera, Pyrrhocoridae). *Journal of Insect Physiology*. 1985;31(5):383-8.
30. Stjernholm F, Karlsson B. Flight muscle breakdown in the green-veined white butterfly, *Pieris napi* (Lepidoptera : Pieridae). *Eur J Entomol*. 2008;105(1):87-91.
31. Bhakthan NM, Borden JH, Nair KK. Fine structure of degenerating and regenerating flight muscles in a bark Beetle, *Ips-Confusus*. I. Degeneration. *Journal of Cell Science*. 1970;6(3):807-19.
32. Bhakthan NM, Nair KK, Borden JH. Fine structure of degenerating and regenerating flight muscles in a bark beetle, *Ips-Confusus*. II. Regeneration. *Can J Zool*. 1971;49(1):85-9.
33. Lee JC, Peter ME. Regulation of apoptosis by ubiquitination. *Immunol Rev*. 2003;193(1):39-47.
34. Gupta I, Singh K, Varshney NK, Khan S. Delineating crosstalk mechanisms of the ubiquitin proteasome system that regulate apoptosis. *Front Cell Dev Biol*. 2018;6.
35. Sun XX, DeVine T, Challagundla KB, Dai MS. Interplay between ribosomal protein S27a and MDM2 protein in p53 activation in response to ribosomal stress. *J Biol Chem*. 2011;286(26):22730-41.
36. Kano R, Kubota A, Nakamura Y, Watanabe S, Hasegawa A. Feline ubiquitin fusion protein genes. *Vet Res Commun*. 2001;25(8):615-22.
37. Feng H, Sun H, Yin J, Li K, Xi J, Cao Y. Progress of molecular biology researches in apoptosis of insect flight muscles. *Chinese Journal of Applied Entomology*. 2011;48(3):701-9.

Supplementary Files

Figure S1 Morphological and histological examinations of wing development in aphid nymphs. (A, a) The external and internal structures in the first instar nymphs under HD and LD conditions are similar. Wing

primordia were observed in the internal structures of nymphs in both conditions. (B, b, b') In the second instar stage, the external structures continued to be similar in nymphs under HD and LD conditions. However, the wing primordia (arrow) developed and enlarged in the winged line and the wing primordia disappeared in the wingless line. (C, C', c, c') Swollen structures were observed on the third instar nymphs under HD conditions, while not in the LD conditions. Swollen structures were identified as the wing bud in the future winged aphids. In the inner structures, the wing primordia continually developed and enlarged in the winged lines. Flight muscles fibers also differentiated. The primordia disappeared in the wingless line, and the area in which the flight muscle develops was occupied by fat bodies. (D, D', d, d') In the fourth instar stage, wing buds enlarged into the shape of a plate. There were no wing buds in the wingless line. The flight muscles of the winged line increased in size and occupied half of the thoracic area. The wing epithelia of the wing buds were folded in a complicated structure. The folding patterns were different between the forewings and hindwings. Fat bodies occupied the corresponding thoracic locations in the wingless aphids. (E) Wing hair sensilla were also seen in the winged line. (F) It shows the wing hair sensilla of the adult wing aphid.

Figure S2 Gel visualization of differentially expressed genes before and after aphid migration. 6% polyacrylamide gel electrophoresis of PCR products from representative DDRT-PCR primer pairs. Arrowhead indicates genes that show different expressions before and after aphid migration.

Figure S3 Alignment (left) and phylogenetic analysis (right) of amino acids sequences of ubiquitin-ribosomal S27a from 18 insects. The tree shown is an observed divergency tree inferred from alignment. Statistical support for each individual node on the tree is shown above the nodes. GreenBox stands for Coleoptera, BlueBox stands for Lepidoptera, YellowBox stands for Diptera and RedBox stands for Hemiptera. *Al Agriotes lineatus* (CAJ01876), *Cg Carabus granulatus* (CAH04347), *Md Micromalthus delibis* (CAJ01880), *Tc Tribolium castaneum* (XP_969023), *Tb Timarcha balearica* (CAJ01881), *Bm Byoxsm mori* (ABM55591), *Px Plutella xylostella* ([P68202](#)), *Pd Papilio dardanus* (CAH04128), *Sf Spodoptera frugiperda* ([P68203](#)), *Se Spodoptera exigua* (Deduced), *Dm Drosophila melanogaster* (NP_476778), *Aa Aedes aegypti*(AAS79344), *Dc Diaphorina citri* (ABG81958) *Ga Graphocephala atropunctata* (DQ445503), *Mh Maconellicoccus hirsutus*(ABM55591), *Of Oncopeltus fasciatus* (ABN54483), *AP Acyrthosiphon pisum* (NP_001155610), *Sa Sitobion avenae* (Deduced).

Table S1 DDRT-PCR primers

Table S2 Primers used for the amplification of Ub-RPS27a sequences

Table S3 Differentially expressed genes after aphid tethered migration

Figures



Figure 1

Breakdown of flight muscles of alatae aphids. Mesothoraces of alatae aphids at various stages were fixed, sectioned at 5 μm thickness and stained on the (A) 1st day, (B) 5th day, (C) 9th day, (D) 11th day, and (E) 13th day after the final ecdysis.



Figure 2

Cross-sections of the mesothoracic flight muscle at various stages. The apoptotic wing degeneration occurs at 7th day after the final ecdysis. All the mesothoraces were sectioned at 5 μm thickness. Images for the TUNEL assays are shown for the 3rd day (A, A'), and 7th day (B, B') after the final ecdysis in both the normal and fasted aphid groups. In each of the group, a positive control sample were included to show the cell apoptosis signals (C, C'). The arrowheads indicate apoptotic cells.

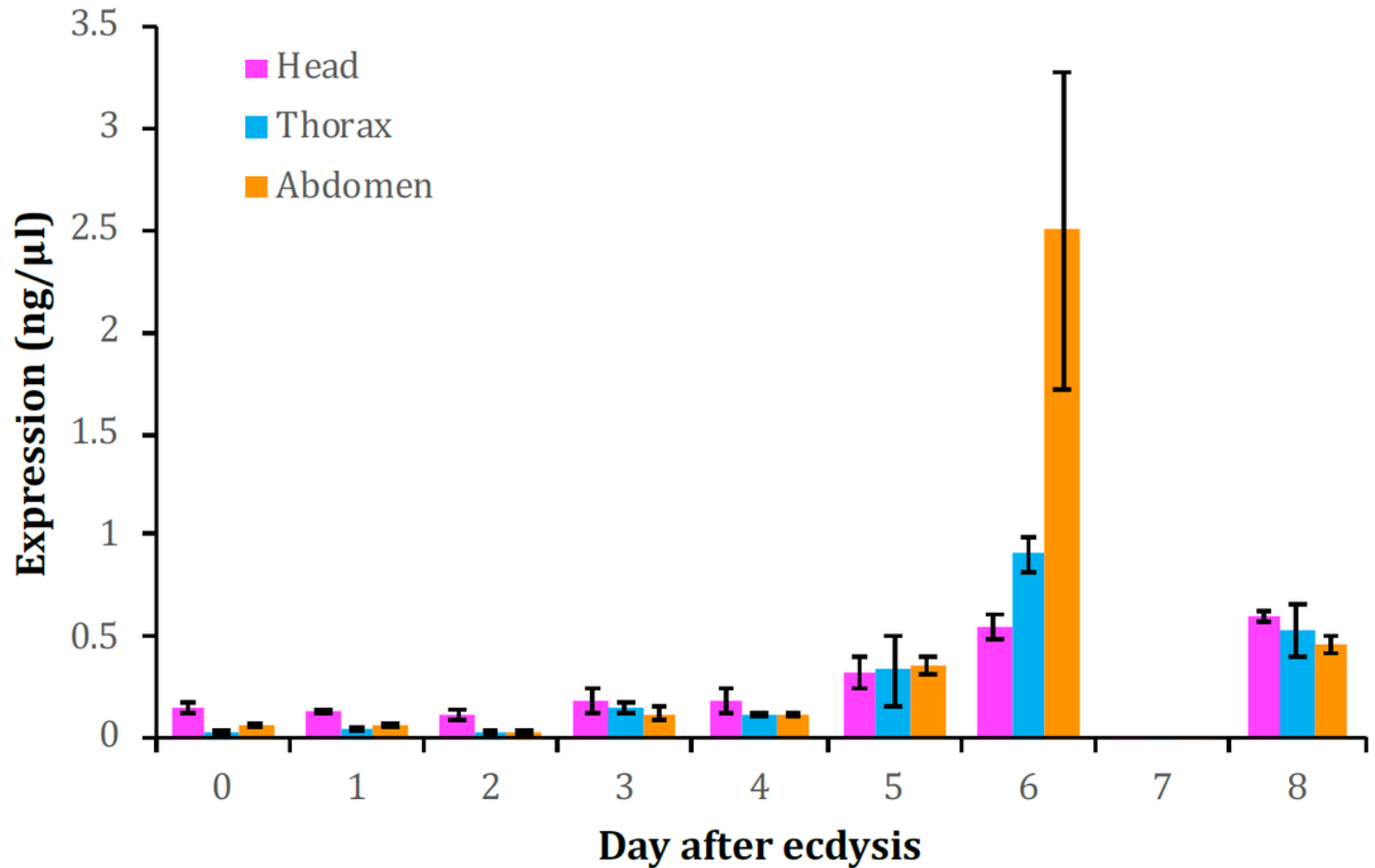


Figure 3

The dynamic expression of *S. avenae* ubiquitin-ribosomal S27a gene. The aphids we collected are from eclosion (0 day) to breeding finished (8th day). The expression in all three tissues always show stable and relatively lower, except a sharp increase in 5th day, with higher in abdomen than in head and thorax. Error bar = \pm Standard Deviation.

Supplementary Files

This is a list of supplementary files associated with this preprint. Click to download.

- [FigS1Final.pdf](#)
- [TableSvFinal.pdf](#)
- [FigS2Final.pdf](#)
- [FigS3Final.pdf](#)